MICS JOURNAL

Mathematics-in-Industry Case Studies Journal, Volume 2, pp. 34-63 (2010)

Modeling of Autothermal Thermophylic Aerobic Digestion

J. Rojas[**] M. Burke[†] M. Chapwanya [*†] K. Doherty [‡] I. Hewitt [§]
A. Korobeinikov[†] M. Meere [¶] S. McCarthy [‖] M. O'Brien[†] V. T. N. Tuoi[‡]
H. Winstanley[†§] T. Zhelev [**]

Abstract. Wastewater treatment requires the elimination of pathogens and reduction of organic matter in the treated sludge to acceptable levels. One process used to achieve this is Autothermal Thermophylic Aerobic Digestion (ATAD), which relies on promoting non-pathogenic thermophilic bacteria to digest organic matter and kill pathogens through metabolic heat generation. This process requires continuous aeration that may be energy consuming, and the final aim of the study is to identify how the process design can minimize the energy input per mass of treated sludge. Appropriate modeling of the reactor process is an essential ingredient, so we explore properties of an existing model and propose a simplified alternative model.

Keywords. Modeling, ATAD, Wastewater treatment, Simulation, Sensitivity analysis

1 Introduction

1.1 Background

Wastewater treatment employs a variety of processes to reduce the environmental and health impacts of effluent. Treatment is an environmental necessity but is itself very energy-intensive, and this energy use is one of the principal costs and environmental impacts of the treatment. Wastewater impurities include a wide range of inorganic and organic chemical species and microorganisms. A filtered, concentrated sludge is produced at initial stages of treatment. A key subsequent stage is to eliminate potential pathogenic organisms and reduce the organic chemical content, which might

[*]Corresponding author. *Email address*: m.chapwanya@ul.ie (Michael Chapwanya)
[†]MACSI, Department of Mathematics and Statistics, University of Limerick, Limerick, Ireland
[‡]National University of Ireland, Galway, Ireland
[§]Mathematical Institute, University of Oxford, 24–29 St Giles', Oxford OX1 3LB, UK
[¶]Department of Applied Mathematics, National University of Ireland, Galway, Ireland
[‖]School of Mathematical Sciences, University College Cork, Cork, Ireland
[**]Department of Chemical and Environmental Science, University of Limerick, Limerick, Ireland. Research funded by Science Foundation Ireland, grant number 06/CP/E007.

act as a substrate for further microbial growth. One process that is used to achieve these treatment goals is autothermal thermophilic aerobic digestion (ATAD). A review of the ATAD origin, design and operation can be found in [10, 12, 13]

ATAD makes use of bacterial growth within the sludge both to reduce organic chemical content and to kill pathogenic bacteria. Aeration of the sludge promotes the growth of aerobic bacteria, which feed on and reduce the organic substrates available in the sludge. This metabolic activity generates heat and raises the temperature of the sludge. Thermophilic bacteria in the sludge thrive at high temperatures (Fig. 1). Most pathogens, meanwhile, are mesophiles: their total metabolic activity reduces rapidly at temperatures above 40 – 45 °C, and they are eventually killed by sufficiently long exposure (Fig. 2). Aerobic thermophiles proliferate and dominate in the hot sludge, and ATAD uses their metabolic activity and heat generation to achieve the treatment goals of pasteurization and reduction of organics.

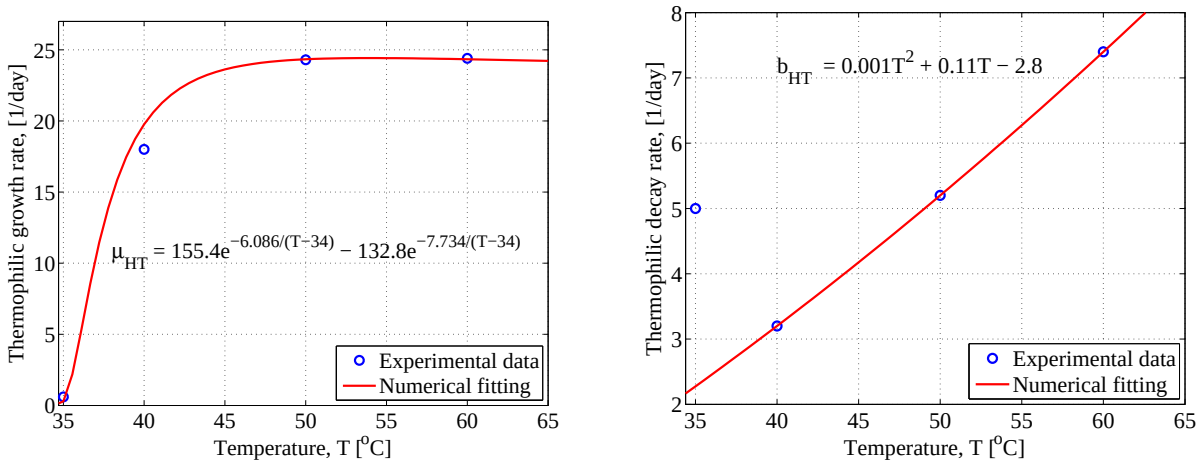

Figure 1: *Temperature dependence of the thermophilic growth rate μ_{HT}, and decay rate b_{HT}. The experimental data and the fitting were adapted from [9].*

The time and cost implications of running full-scale experiments for different plant arrangements and operating conditions render such an approach infeasible for process design and operational management. Laboratory scale experiments have provided understanding (to varying degree) of many of the microbiological and chemical processes involved. By encapsulating much of this understanding in mathematical models, engineers have provided tools that allow computer simulations to inform the design process. The 'Activated Sludge Model 1' (ASM1) [7] and subsequent variants [5, 6] have achieved a broad level of acceptance in the wastewater treatment world. Based on the dominance of the ASM1 model (and family) in the field, its extension to the ATAD process as set out by [8, 4] appears to have created a *de facto* standard for modeling this process, despite drawbacks summarized below. We identify this existing model with the label ASM1.

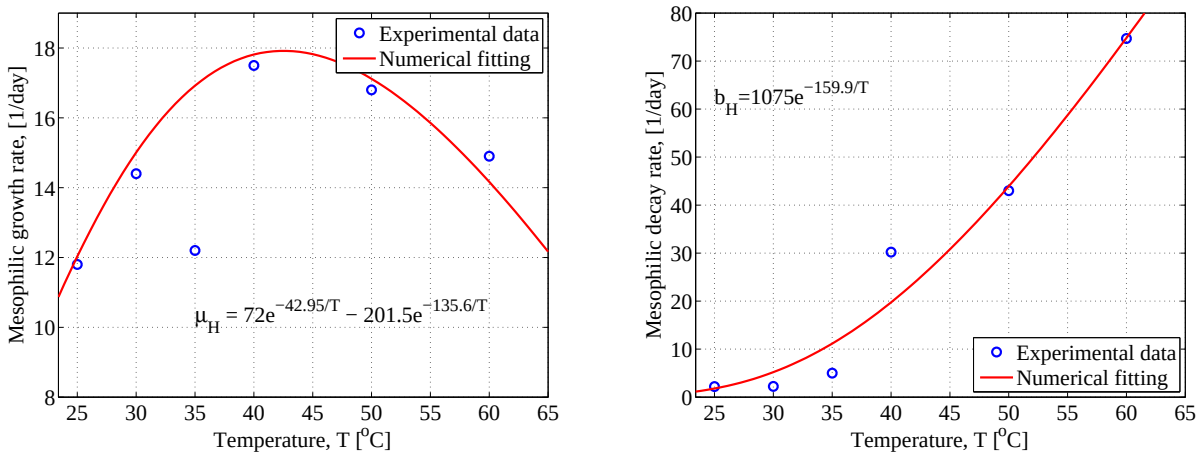

Figure 2: *Temperature dependence of the mesophilic growth rate μ_H, and decay rate b_H. The experimental data and the fitting were adapted from [9].*

1.2 Treatment Plant and Process

ATAD is operated as a batch or semi-batch process. A large reactor containing sludge receives an additional volume of untreated sludge at the start of a batch via a feed inlet (see schematic in Fig. 4). During the batch reaction air is pumped continuously into the reactor and provides both the oxygenation required for aerobic bacterial growth and the physical mixing of the sludge in the whole reactor. Digestion of organic substrates proceeds hand in hand with bacterial growth, predominantly of thermophiles due to the elevated temperature. At the end of the batch reaction time, a volume of treated outflow sludge is removed and is immediately replaced by the next batch of intake sludge. Thus the outflow sludge has the same composition as the mixed sludge in the reactor at the end of the batch reaction time t_{batch}. Batch outflow and inflow cannot be open at the same time since untreated inflow sludge might be drawn off with and taint the outflow sludge. The time between successive batch intakes is typically fixed at 24 hours for staffing reasons. In order to achieve the desired treatment outcomes, treatment plant designs may include a single ATAD reactor stage, or two reactors in series with outflow from the first reactor being inflow into the second. In some cases, the treatment plant consists of an ATAD reactor and an anaerobic mesophilic digester in series (cf. [11]). The method of operation and the number of reactors used depends on the fluctuation of hydraulic loading and on the quantity of sludge requiring treatment.

1.3 Objective

Our ultimate goal is the optimization of ATAD systems. In this context, developing a simple and computationally efficient model is critical. Thus, the main objective of this paper is to develop a simplified model of the ATAD reaction based on the existing ASM1 model at thermophilic temperatures (see for example [9], [14]).

(a) (b)

Figure 3: *(a) Stand-alone reactor plant; (b) Two reactor in series design. The two designs displayed correspond to plants located in Tudela (Navarra, Spain) and Killarney (Co. Kerry, Ireland), respectively.*

The key focus of this paper is modeling the core process of a single reactor system during a batch. Such a model is trivially set up to run successive batches and can easily be extended later to a multi-reactor system and other design variants. We will present a sensitivity analysis and investigate the existing ASM1 model. We will focus on a single reactor system of fixed design, with plant design optimization left as a task for future work.

The rest of this paper is structured as follows: starting in Section 2, we provide a detailed overview of the problem. In Section 3 we discuss the ASM1 model, perform a nondimensionalization based on typical parameter values (adapted from [4] and [8]), and identify certain regimes within the timecourse of a single typical batch reaction for which asymptotic approximations may be appropriate. In Section 4 we present a simplified model with the intention of being the minimal model required to describe the observed process. The model comprises a system of ODEs with four dependent variables. In Section 5 we compare our simulations to experiments and present a sensitivity analysis of the derived model. In Section 6 we discuss the formulation of the optimization problem which will be implemented in a future publication.

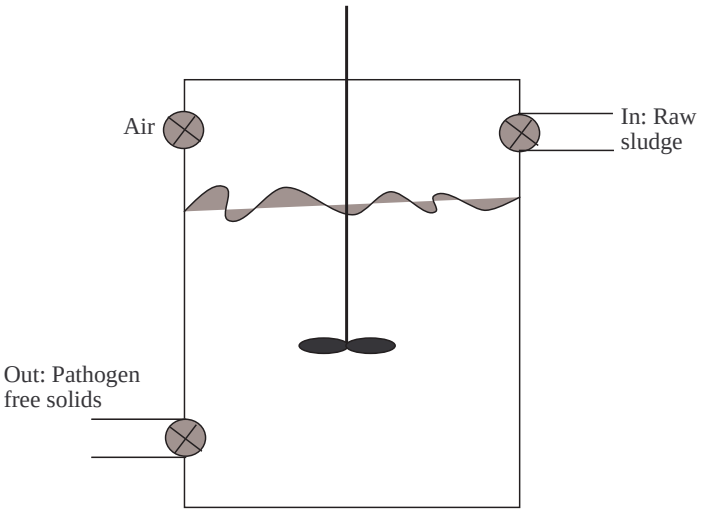

Figure 4: *Schematic representation of a reactor. The ATAD process must have a feed control mechanism which ensures that the organic feed is above a certain minimum concentration for adequate heat production. The solids must also be below a maximum concentration to allow adequate mixing. See for example [11].*

2 Problem Overview

Existing models are far too large and complex, and this complexity prevent the application of the usual optimization techniques. Our aim is to construct a simple model that retain the fundamental properties of the large scale existing models while being simple enough to allow the use of optimization procedures.

2.1 Treatment Goals

Legal requirements for sludge treatment in Ireland and USA set minimum standards for the pasteurization and stabilization of the treated outflow sludge [11]. Stabilization refers to the reduction of volatile solids concentration between sludge intake $X_{\text{vs}}^{\text{feed}}$ and outflow $X_{\text{vs}}^{\text{out}}$, and the required minimum reduction is set at 38% [16]:

$$r_{\text{vs}} = \frac{X_{\text{vs}}^{\text{feed}} - X_{\text{vs}}^{\text{out}}}{X_{\text{vs}}^{\text{feed}}} \quad \geq \quad 0.38. \tag{1}$$

Pasteurization is achieved by the sludge being subjected to high temperature for a prolonged period of time. Rather than requiring direct microbiological testing of the outflow, the legal requirement for pasteurization specifies a minimum value of 1.0 for a derived 'lethality' statistic, which is an

empirically-based function of sludge temperature, and time elapsed in the ATAD reaction process:

$$L(T,t) \;=\; \int_{t_0}^{t} \frac{1}{a}\, 10^{bT(s)}\, ds \quad \geq \quad 1, \tag{2}$$

where temperature T is measured in Celsius, elapsed time t in days, and $a = 5.007 \times 10^7$ *days* and $b = [0.14\,^{\circ}\mathrm{C}]^{-1}$ are defined parameter values. Lethality L is calculated in continuous time intervals where $T \geq 50\,^{\circ}\mathrm{C}$, and it is assumed to be zero when $T < 50\,^{\circ}\mathrm{C}$, [16].

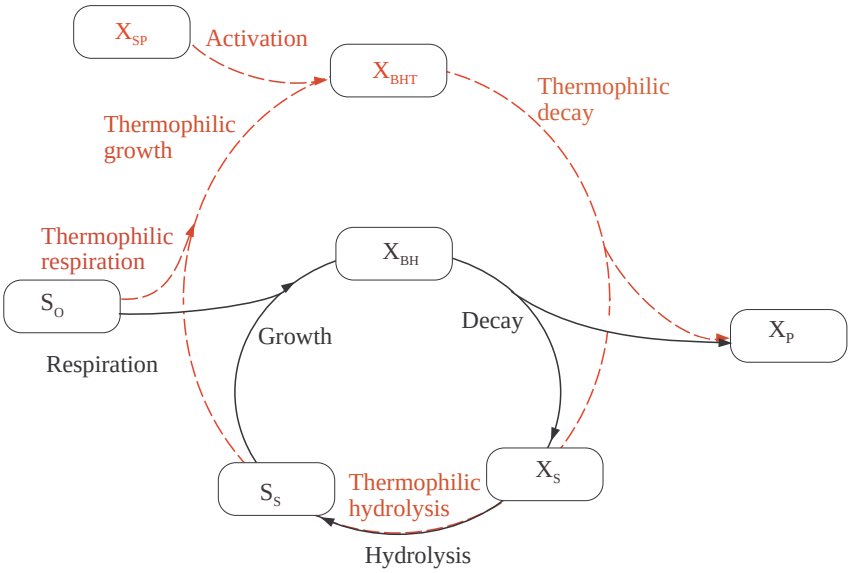

Figure 5: *Mass cycle diagram of the processes in the ASM1 model (solid lines) and the proposed extended model (broken lines). In Section 3.1 we present the mathematical representation of the extended model. (adapted from [9])*

3 The ASM1 Model

The ASM1 model incorporates all the processes identified by microbiologists as being relevant to modeling the ATAD process. The mass cycle diagram of the ASM1 model is shown in Fig. 5 with the solid curve cycle showing the processes included in the original ASM1 model (prior to the ATAD extension). Here X_{BH} denotes the concentration of active mesophilic biomass, S_{O} is the concentration of oxygen and X_{P} is the concentration of inert organic matter. Organic substrate is separated into readily biodegradable substrate S_{S} and slowly degradable substrate X_{S}. Untreated sludge in the batch inflow contains a certain concentration of both these substrates. The slow substrate X_{S} consists of organic macromolecules which can be hydrolyzed to produce the fast substrate S_{S}. Microbial decay adds to the pool of X_{S}: cell lysis on death releases the cell's constituents into the

extracellular space, a fraction f_{P} of which is inert matter and $(1-f_{\mathrm{P}})$ is hydrolyzable macromolecular substrate. Fast substrate S_{S} and oxygen S_{O} are consumed in growth of the bacteria. All the metabolic process rates are assumed to depend nonlinearly on substrate and oxygen concentrations through dual Michaelis–Menten kinetics terms.

The ATAD-specific modifications to the ASM1 model are (broken curve cycle in Fig. 5) via the introduction of a new component: thermophilic biomass, in active X_{BHT} and inactive X_{SP} forms. While mesophiles are relevant to batch reactions starting from cold, typical ATAD plants are operated with batches following in rapid succession precisely in order to maintain the temperature of the reactor. Under these conditions, the mesophiles respire but the temperatures are beyond their optimum level and so they decay very fast and thus do not make noticeable contribution to the process, see Fig. 2.

3.1 The ASM1 Model at Thermophilic Temperatures

The ASM1 model at thermophilic temperatures tracks the evolution in time of eight quantities in the reactor. For simplicity, we disregard the temperature dependence here, and so do not display an equation for the temperature. We take fixed values for the model parameters and choose these values for reactor operation at 50°C. We also neglect the effect of thermophilic activation, on the basis that it occurs rapidly at the start of the batch reaction, and so do not consider inactive biomass X_{SP} in the model. Under these assumptions, the governing equations from [8] are

$$
\begin{aligned}
\frac{dS_{\mathrm{S}}}{dt} &= -\frac{1}{Y_{\mathrm{H}}}\mu_{\mathrm{H}}\frac{S_{\mathrm{S}}}{K_{\mathrm{S}}+S_{\mathrm{S}}}\frac{S_{\mathrm{O}}}{K_{\mathrm{O}}+S_{\mathrm{O}}}X_{\mathrm{BH}} - \frac{1}{Y_{\mathrm{HT}}}\mu_{\mathrm{HT}}\frac{S_{\mathrm{S}}}{K_{\mathrm{ST}}+S_{\mathrm{S}}}\frac{S_{\mathrm{O}}}{K_{\mathrm{OT}}+S_{\mathrm{O}}}X_{\mathrm{BHT}} \\
&\quad + k_{\mathrm{H}}\frac{X_{\mathrm{S}}}{K_{\mathrm{X}}X_{\mathrm{BH}}+X_{\mathrm{S}}}\frac{S_{\mathrm{O}}}{K_{\mathrm{O}}+S_{\mathrm{O}}}X_{\mathrm{BH}} + k_{\mathrm{HT}}\frac{X_{\mathrm{S}}}{K_{\mathrm{XT}}X_{\mathrm{BHT}}+X_{\mathrm{S}}}\frac{S_{\mathrm{O}}}{K_{\mathrm{OT}}+S_{\mathrm{O}}}X_{\mathrm{BHT}}, \\
\frac{dX_{\mathrm{S}}}{dt} &= b_{\mathrm{H}}(1-f_P)X_{\mathrm{BH}} + b_{\mathrm{HT}}(1-f_{\mathrm{PT}})X_{\mathrm{BHT}} - k_{\mathrm{H}}\frac{X_{\mathrm{S}}}{K_{\mathrm{X}}X_{\mathrm{BH}}+X_{\mathrm{S}}}\frac{S_{\mathrm{O}}}{K_{\mathrm{O}}+S_{\mathrm{O}}}X_{\mathrm{BH}} \\
&\quad - k_{\mathrm{HT}}\frac{X_{\mathrm{S}}}{K_{\mathrm{XT}}X_{\mathrm{BHT}}+X_{\mathrm{S}}}\frac{S_{\mathrm{O}}}{K_{\mathrm{OT}}+S_{\mathrm{O}}}X_{\mathrm{BHT}}, \\
\frac{dX_{\mathrm{BH}}}{dt} &= \mu_{\mathrm{H}}\frac{S_{\mathrm{S}}}{K_{\mathrm{S}}+S_{\mathrm{S}}}\frac{S_{\mathrm{O}}}{K_{\mathrm{O}}+S_{\mathrm{O}}}X_{\mathrm{BH}} - b_{\mathrm{H}}X_{\mathrm{BH}}, \\
\frac{dX_{\mathrm{BHT}}}{dt} &= \mu_{\mathrm{HT}}\frac{S_{\mathrm{S}}}{K_{\mathrm{ST}}+S_{\mathrm{S}}}\frac{S_{\mathrm{O}}}{K_{\mathrm{OT}}+S_{\mathrm{O}}}X_{\mathrm{BHT}} - b_{\mathrm{HT}}X_{\mathrm{BHT}}, \\
\frac{dS_{\mathrm{O}}}{dt} &= -\frac{(1-Y_{\mathrm{H}})}{Y_{\mathrm{H}}}\mu_{\mathrm{H}}\frac{S_{\mathrm{S}}}{K_{\mathrm{S}}+S_{\mathrm{S}}}\frac{S_{\mathrm{O}}}{K_{\mathrm{O}}+S_{\mathrm{O}}}X_{\mathrm{BH}} - \frac{(1-Y_{\mathrm{HT}})}{Y_{\mathrm{HT}}}\mu_{\mathrm{HT}}\frac{S_{\mathrm{S}}}{K_{\mathrm{ST}}+S_{\mathrm{S}}}\frac{S_{\mathrm{O}}}{K_{\mathrm{OT}}+S_{\mathrm{O}}}X_{\mathrm{BHT}} \\
&\quad + k_{La}\left(\bar{S_{\mathrm{O}}}-S_{\mathrm{O}}\right), \\
\frac{dX_{\mathrm{P}}}{dt} &= f_P k_{\mathrm{H}}\frac{X_{\mathrm{S}}}{K_{\mathrm{X}}X_{\mathrm{BH}}+X_{\mathrm{S}}}\frac{S_{\mathrm{O}}}{K_{\mathrm{O}}+S_{\mathrm{O}}}X_{\mathrm{BH}} + f_{\mathrm{PT}}k_{\mathrm{HT}}\frac{X_{\mathrm{S}}}{K_{\mathrm{XT}}X_{\mathrm{BHT}}+X_{\mathrm{S}}}\frac{S_{\mathrm{O}}}{K_{\mathrm{OT}}+S_{\mathrm{O}}}X_{\mathrm{BHT}}.
\end{aligned}
\tag{3}
$$

The parameters appearing in the model are explained in Table 1. We see that the first five of these equations can be solved independently of the sixth, and so we do not display the equation for the inert organic matter X_{P} again.

We model the operation of a single tank system for one batch, and so solve $(3)_1$ – $(3)_5$ subject

to initial conditions

$$S_{\rm S} = S_{\rm S}^o,\ X_{\rm S} = X_{\rm S}^o,\ X_{\rm BH} = X_{\rm BH}^o,\ X_{\rm BHT} = X_{\rm BHT}^o,\ S_{\rm O} = S_{\rm O}^o \quad \text{at} \quad t = 0. \tag{4}$$

For the illustrative numerical results used in the current analysis, we take

$$S_{\rm S}^o = 5\ \text{gl}^{-1},\ X_{\rm S}^o = 15\ \text{gl}^{-1},\ X_{\rm BH}^o = 1\ \text{gl}^{-1},\ X_{\rm BHT}^o = 1\ \text{gl}^{-1},\ S_{\rm O}^o = 10^{-3}\ \text{gl}^{-1}.$$

We scale the system of ordinary differential equations by choosing

$$t \sim t_{\rm batch},\ S_{\rm S} \sim S_{\rm S}^o,\ X_{\rm S} \sim X_{\rm S}^o,\ X_{\rm BH} \sim X_{\rm BH}^o,\ X_{\rm BHT} \sim X_{\rm BHT}^o,\ S_{\rm O} \sim S_{\rm O}^o,$$

where $t_{\rm batch} = 1$ d (one day). With this choice of scaling, the dimensionless form for $(3)_1$–$(3)_5$, (4) is given by,

$$\begin{aligned}
\frac{dS_{\rm S}}{dt} &= -\delta_1 \frac{S_{\rm S}}{\delta_2 + S_{\rm S}} \frac{S_{\rm O}}{\delta_3 + S_{\rm O}} X_{\rm BH} - \delta_4 \frac{S_{\rm S}}{\delta_5 + S_{\rm S}} \frac{S_{\rm O}}{\delta_6 + S_{\rm O}} X_{\rm BHT} \\
&\quad + \delta_7 \frac{X_{\rm S}}{\delta_8 X_{\rm BH} + X_{\rm S}} \frac{S_{\rm O}}{\delta_3 + S_{\rm O}} X_{\rm BH} + \delta_9 \frac{X_{\rm S}}{\delta_{10} X_{\rm BHT} + X_{\rm S}} \frac{S_{\rm O}}{\delta_6 + S_{\rm O}} X_{\rm BHT}, \\
\frac{dX_{\rm S}}{dt} &= \delta_{11} X_{\rm BH} + \delta_{12} X_{\rm BHT} - \delta_{13} \frac{X_{\rm S}}{\delta_8 X_{\rm BH} + X_{\rm S}} \frac{S_{\rm O}}{\delta_3 + S_{\rm O}} X_{\rm BH} - \delta_{14} \frac{X_{\rm S}}{\delta_{10} X_{\rm BHT} + X_{\rm S}} \frac{S_{\rm O}}{\delta_6 + S_{\rm O}} X_{\rm BHT}, \\
\frac{dX_{\rm BH}}{dt} &= \delta_{15} \frac{S_{\rm S}}{\delta_2 + S_{\rm S}} \frac{S_{\rm O}}{\delta_3 + S_{\rm O}} X_{\rm BH} - \delta_{16} X_{\rm BH}, \\
\frac{dX_{\rm BHT}}{dt} &= \delta_{17} \frac{S_{\rm S}}{\delta_5 + S_{\rm S}} \frac{S_{\rm O}}{\delta_6 + S_{\rm O}} X_{\rm BHT} - \delta_{18} X_{\rm BHT}, \\
\frac{dS_{\rm O}}{dt} &= -\delta_{19} \frac{S_{\rm S}}{\delta_2 + S_{\rm S}} \frac{S_{\rm O}}{\delta_3 + S_{\rm O}} X_{\rm BH} - \delta_{20} \frac{S_{\rm S}}{\delta_5 + S_{\rm S}} \frac{S_{\rm O}}{\delta_6 + S_{\rm O}} X_{\rm BHT} + \delta_{21} \left(\delta_{22} - S_{\rm O}\right),
\end{aligned} \tag{5}$$

subject to initial conditions

$$S_{\rm S} = 1,\ X_{\rm S} = 1,\ X_{\rm BH} = 1,\ X_{\rm BHT} = 1,\ S_{\rm O} = 1 \quad \text{at} \quad t = 0,$$

where the definition of, and values for, the non-dimensional parameters δ_i $(1 \le i \le 22)$ are given in Table 2.

In Fig. 6, we show the solution to the system of equations (5) for the parameter values listed in Table 2. It is noteworthy from the parameter values chosen, the readily degradable material is depleted over a period of approximately one half of a day, but that the slowly degradable material persists for approximately five days. We should note, however, that that some of the parameter values used are uncertain, and that they can depend on temperature and time, as well as other factors, such as the character of the inflow sludge and the reactor system. Since we have assumed the parameter values to be fixed, the limitations of such an approach are clear. However, our goal in this section is to gain some insight into aspects of the ASM1 model, rather than attempting to model a particular reactor system in detail.

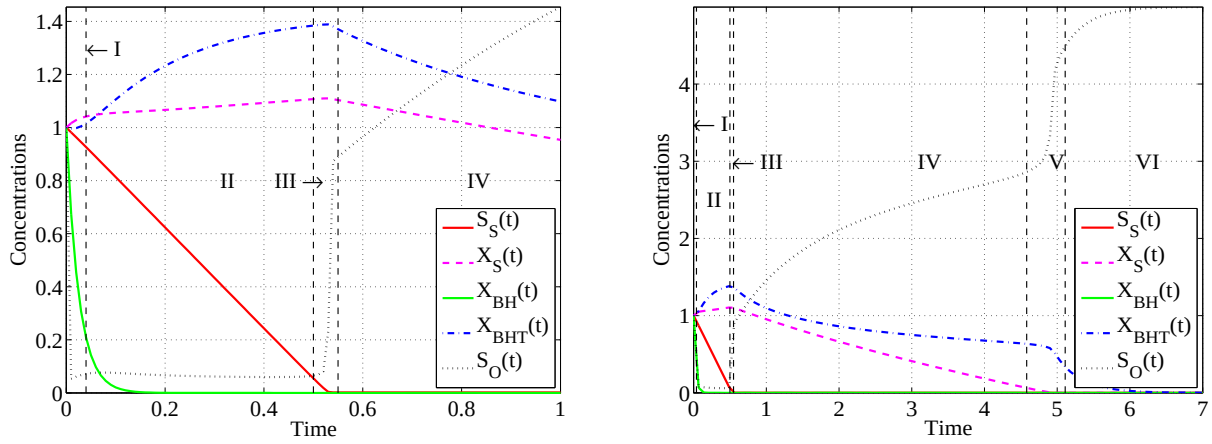

Figure 6: *(a) Plot of the solution to system of equations (5) over one day and for the parameter values displayed in Table 2. (b) The same solution as in (a) plotted over one week. Over this time, the slowly biodegradable substrate is removed, and the dissolved oxygen achieves its saturation value.*

3.2 Asymptotic Analysis of the ASM1 Model

As mentioned above, under normal ATAD operating conditions a relatively high temperature is maintained in the reactor. Commonly, the temperature after adding a new inflow batch and mixing remains higher than the mesophilic temperature range, and hence their metabolic activity is negligible. Therefore we neglect mesophiles in the model and set $X_{\rm BH} = 0$; equations (5) then reduce to

$$\begin{aligned}
\frac{dS_{\rm S}}{dt} &= -\delta_4 \frac{S_{\rm S}}{\delta_5 + S_{\rm S}} \frac{S_{\rm O}}{\delta_6 + S_{\rm O}} X_{\rm BHT} + \delta_9 \frac{X_{\rm S}}{\delta_{10} X_{\rm BHT} + X_{\rm S}} \frac{S_{\rm O}}{\delta_6 + S_{\rm O}} X_{\rm BHT}, \\
\frac{dX_{\rm S}}{dt} &= \delta_{12} X_{\rm BHT} - \delta_{14} \frac{X_{\rm S}}{\delta_{10} X_{\rm BHT} + X_{\rm S}} \frac{S_{\rm O}}{\delta_6 + S_{\rm O}} X_{\rm BHT}, \\
\frac{dX_{\rm BHT}}{dt} &= \delta_{17} \frac{S_{\rm S}}{\delta_5 + S_{\rm S}} \frac{S_{\rm O}}{\delta_6 + S_{\rm O}} X_{\rm BHT} - \delta_{18} X_{\rm BHT}, \\
\frac{dS_{\rm O}}{dt} &= -\delta_{20} \frac{S_{\rm S}}{\delta_5 + S_{\rm S}} \frac{S_{\rm O}}{\delta_6 + S_{\rm O}} X_{\rm BHT} + \delta_{21} \left(\delta_{22} - S_{\rm O}\right), \\
S_{\rm S} &= 1,\ X_{\rm S} = 1,\ X_{\rm BHT} = 1,\ S_{\rm O} = 1 \quad \text{at} \quad t = 0.
\end{aligned} \tag{6}$$

In Fig. 7, we display numerical solutions of system of equations (6) for the parameter values given in Table 2. Comparing these with the solutions given in Fig. 6, one notes that there is good qualitative agreement and reasonable quantitative agreement, as would be expected.

Motivated by the relevant parameter values listed in Table 2, we denote

$$\delta_5 = \varepsilon,\ \delta_{10} = \theta_1 \varepsilon,\ \delta_{20} = \theta_2/\varepsilon,\ \delta_{21} = \theta_3/\varepsilon,$$

Table 1: *The set of parameters for the ASM1 model. Experiments have shown that these parameters can depend, among other things, on temperature and time (see Figs. 1 and 2). Here we assume these parameters to be constant (i.e., temperature independent).*

Symbol	Description	Value	Units
	Physical parameters		
K_{S}	mesophilic half saturation constant for S_{S}	0.02	g/l
K_{O}	mesophilic half saturation constant for S_{O}	2×10^{-4}	g/l
K_{ST}	thermophilic half saturation constant for S_{S}	0.03	g/l
K_{OT}	thermophilic half saturation constant for S_{O}	2×10^{-4}	g/l
$\bar{S_{\mathrm{O}}}$	oxygen saturation concentration	5×10^{-3}	g/l
μ_{H}	maximum growth rate of X_{BH}	16.8	1/d
μ_{HT}	maximum growth rate of X_{BHT}	24.3	1/d
b_{H}	decay rate of mesophiles	43	1/d
b_{HT}	decay rate of thermophiles	5.2	1/d
k_{H}	maximum mesophilic hydrolysis rate	10	1/d
k_{HT}	maximum thermophilic hydrolysis rate	9.2	1/d
k_{La}	oxygen mass transfer coefficient	1000	1/d
Y_{H}	mesophilic yield	0.6	–
Y_{HT}	thermophilic yield	0.6	–
f_P	inert fraction of mesophilic biomass	0.3	–
f_{PT}	inert fraction of thermophilic biomass	0.3	–
K_{X}	half saturation constant for mesophilic hydrolysis	0.03	–
K_{XT}	half saturation constant for thermophilic hydrolysis	0.03	–

where $\theta_1, \theta_2, \theta_3 = \mathcal{O}(1)$, and consider the limit $\varepsilon \to 0$. This correspond to a limit where there is no dependence on S_{S}, i.e., growth is not inhibited by the substrate. For reference, it is worth re-displaying equations (6) now in terms of the parameter ε

$$
\begin{aligned}
&\frac{dS_{\mathrm{S}}}{dt} = -\delta_4 \frac{S_{\mathrm{S}}}{\varepsilon + S_{\mathrm{S}}} \frac{S_{\mathrm{O}}}{\delta_6 + S_{\mathrm{O}}} X_{\mathrm{BHT}} + \delta_9 \frac{X_{\mathrm{S}}}{\theta_1 \varepsilon X_{\mathrm{BHT}} + X_{\mathrm{S}}} \frac{S_{\mathrm{O}}}{\delta_6 + S_{\mathrm{O}}} X_{\mathrm{BHT}},\\
&\frac{dX_{\mathrm{S}}}{dt} = \delta_{12} X_{\mathrm{BHT}} - \delta_{14} \frac{X_{\mathrm{S}}}{\theta_1 \varepsilon X_{\mathrm{BHT}} + X_{\mathrm{S}}} \frac{S_{\mathrm{O}}}{\delta_6 + S_{\mathrm{O}}} X_{\mathrm{BHT}},\\
&\frac{dX_{\mathrm{BHT}}}{dt} = \delta_{17} \frac{S_{\mathrm{S}}}{\varepsilon + S_{\mathrm{S}}} \frac{S_{\mathrm{O}}}{\delta_6 + S_{\mathrm{O}}} X_{\mathrm{BHT}} - \delta_{18} X_{\mathrm{BHT}},\\
&\varepsilon \frac{dS_{\mathrm{O}}}{dt} = -\theta_2 \frac{S_{\mathrm{S}}}{\varepsilon + S_{\mathrm{S}}} \frac{S_{\mathrm{O}}}{\delta_6 + S_{\mathrm{O}}} X_{\mathrm{BHT}} + \theta_3 \left(\delta_{22} - S_{\mathrm{O}}\right),\\
&S_{\mathrm{S}} = 1,\ X_{\mathrm{S}} = 1,\ X_{\mathrm{BHT}} = 1,\ S_{\mathrm{O}} = 1 \quad \text{at} \quad t = 0.
\end{aligned}
\tag{7}
$$

Table 2: *Dimensionless set of parameters for the ASM1 model.*

Symbol	Description	Value
δ_1	$\mu_{\mathrm{H}} t_{\mathrm{batch}} X^o_{\mathrm{BH}}/(Y_{\mathrm{HT}} S^o_{\mathrm{S}})$	5.60
δ_2	$K_{\mathrm{S}}/S^o_{\mathrm{S}}$	4×10^{-3}
δ_3	$K_{\mathrm{O}}/S^o_{\mathrm{O}}$	0.2
δ_4	$\mu_{\mathrm{HT}} t_{\mathrm{batch}} X^o_{\mathrm{BHT}}/(Y_{\mathrm{HT}} S^o_{\mathrm{S}})$	8.10
δ_5	$K_{\mathrm{ST}}/S^o_{\mathrm{S}}$	6×10^{-3}
δ_6	$K_{\mathrm{OT}}/S^o_{\mathrm{O}}$	0.2
δ_7	$k_{\mathrm{H}} t_{\mathrm{batch}} X^*_{\mathrm{BH}}/S^*_{\mathrm{S}}$	2.0
δ_8	$K_{\mathrm{X}} X^o_{\mathrm{BH}}/X^o_{\mathrm{S}}$	2×10^{-3}
δ_9	$(k_{\mathrm{HT}} t_{\mathrm{batch}})\,(X^*_{\mathrm{BHT}}/S^o_{\mathrm{S}})$	1.84
δ_{10}	$K_{\mathrm{XT}} X^o_{\mathrm{BHT}}/X^o_{\mathrm{S}}$	2×10^{-3}
δ_{11}	$(1-f_{\mathrm{P}}) b_{\mathrm{H}} t_{\mathrm{batch}} X^o_{\mathrm{BH}}/X^o_{\mathrm{S}}$	2.01
δ_{12}	$(1-f_{\mathrm{PT}}) b_{\mathrm{HT}} t_{\mathrm{batch}} X^o_{\mathrm{BHT}}/X^o_{\mathrm{S}}$	0.25
δ_{13}	$k_{\mathrm{H}} t_{\mathrm{batch}} X^o_{\mathrm{BH}}/X^o_{\mathrm{S}}$	0.67
δ_{14}	$k_{\mathrm{HT}} t_{\mathrm{batch}} X^o_{\mathrm{BHT}}/X^o_{\mathrm{S}}$	0.61
δ_{15}	$\mu_{\mathrm{H}} t_{\mathrm{batch}}$	16.8
δ_{16}	$b_{\mathrm{H}} t_{\mathrm{batch}}$	43.0
δ_{17}	$\mu_{\mathrm{HT}} t_{\mathrm{batch}}$	24.3
δ_{18}	$b_{\mathrm{HT}} t_{\mathrm{batch}}$	5.2
δ_{19}	$(1-Y_{\mathrm{H}}) \mu_{\mathrm{H}} t_{\mathrm{batch}} X^o_{\mathrm{BH}}/(Y_{\mathrm{H}} S^o_{\mathrm{O}})$	11.2×10^3
δ_{20}	$(1-Y_{\mathrm{HT}}) \mu_{\mathrm{HT}} t_{\mathrm{batch}} X^o_{\mathrm{BHT}}/(Y_{\mathrm{HT}} S^o_{\mathrm{O}})$	16.2×10^3
δ_{21}	$k_{La} t_{\mathrm{batch}}$	10^3
δ_{22}	$\bar{S_{\mathrm{O}}}/S^o_{\mathrm{O}}$	5.0

The limit $\varepsilon \to 0$ is singular, and the asymptotic structure is indicated in Fig. 7. We now briefly discuss some of the asymptotic regions (time-scales) arising.

3.3 Region I, $t = \mathcal{O}(\varepsilon)$

The very short initial time-scale which is visible in Fig. 7(a) and Fig. 7(b), although barely visible in Fig. 7(b), appears at $t = \mathcal{O}(\varepsilon)$ and marks a region of rapid change in the dissolved oxygen concentration. We rescale $t = \varepsilon \hat{t}$, and at leading order we have

$$S_{\mathrm{S}} \sim 1, \; X_{\mathrm{S}} \sim 1, \; X_{\mathrm{BHT}} \sim 1,$$

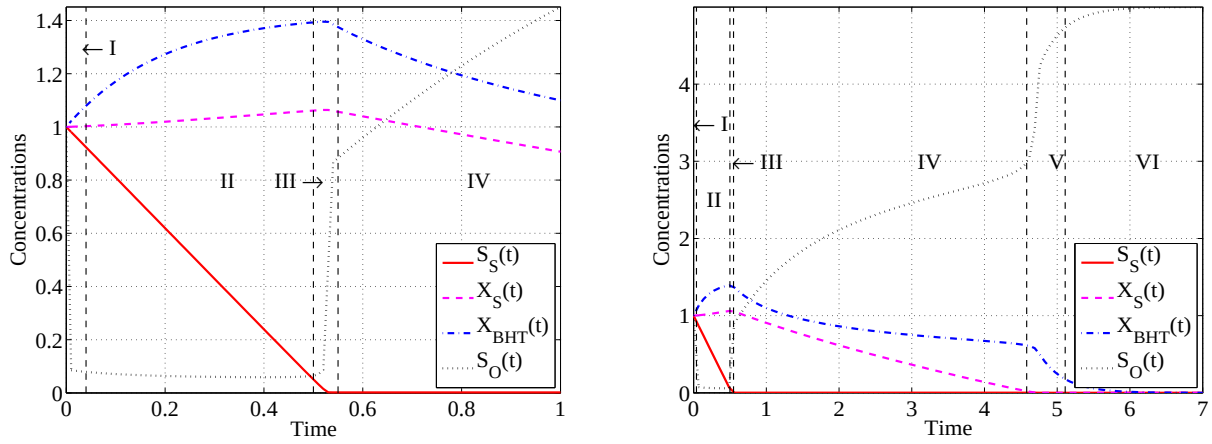

Figure 7: *(a) Plot of the solution to system of equations (6) over one day for the parameter values displayed in Table 2. (b) The same solution as in (a) plotted over one week. The asymptotic regions for $\varepsilon \to 0$ are indicated.*

and pose $S_{\mathrm{O}} \sim S_{\mathrm{O}}^{\mathrm{I}}(\hat{t})$, to obtain

$$\frac{dS_{\mathrm{O}}^{\mathrm{I}}}{d\hat{t}} = -\theta_2 \frac{S_{\mathrm{O}}^{\mathrm{I}}}{\delta_6 + S_{\mathrm{O}}^{\mathrm{I}}} + \theta_3 \left(\delta_{22} - S_{\mathrm{O}}^{\mathrm{I}}\right),$$

where

$$S_{\mathrm{O}}^{\mathrm{I}} = 1 \text{ at } \hat{t} = 0,$$

and $dS_{\mathrm{O}}^{\mathrm{I}}/d\hat{t} \to 0$, $S_{\mathrm{O}}^{\mathrm{I}} \to \rho_1$ as $\hat{t} \to \infty$, with ρ_1 given by

$$\rho_1 = \frac{1}{2}\left(\delta_{22} - \delta_6 - \frac{\theta_2}{\theta_3} + \sqrt{\left(\delta_{22} - \delta_6 - \frac{\theta_2}{\theta_3}\right)^2 + 4\delta_{22}\delta_6}\right).$$

For the parameter values given in Table 2, $\rho_1 = 0.087$, which is in good agreement with the numerical solution displayed in Fig. 7(a). We have to note that $\rho_1 > 1$ is also possible, so that the dissolved oxygen is not necessarily depleted over this time-scale; the competing effects of aeration and oxygen consumption by the biomass enter at leading order here.

3.4 Region II, $t = \mathcal{O}(1)$ and $t < t_{\mathrm{s}}$

For $t = \mathcal{O}(1)$ and $t < t_{\mathrm{s}}$, where t_{s} is the moment when the availability of S_{S} becomes a limiting factor in the further growth of the biomass, we pose

$$S_{\mathrm{S}} \sim S_{\mathrm{S}}^{\mathrm{II}}(t), X_{\mathrm{S}} \sim X_{\mathrm{S}}^{\mathrm{II}}(t), X_{\mathrm{BHT}} \sim X_{\mathrm{BHT}}^{\mathrm{II}}(t), S_{\mathrm{O}} \sim S_{\mathrm{O}}^{\mathrm{II}}(t),$$

for $\varepsilon \to 0$, to obtain

$$\begin{aligned}
\frac{dS_{\rm S}^{\rm II}}{dt} &= -\left(\delta_4 - \delta_9\right) \frac{S_{\rm O}^{\rm II}}{\delta_6 + S_{\rm O}^{\rm II}} X_{\rm BHT}^{\rm II}, \\
\frac{dX_{\rm S}^{\rm II}}{dt} &= \delta_{12} X_{\rm BHT}^{\rm II} - \delta_{14} \frac{S_{\rm O}^{\rm II}}{\delta_6 + S_{\rm O}^{\rm II}} X_{\rm BHT}^{\rm II}, \\
\frac{dX_{\rm BHT}^{\rm II}}{dt} &= \delta_{17} \frac{S_{\rm O}^{\rm II}}{\delta_6 + S_{\rm O}^{\rm II}} X_{\rm BHT}^{\rm II} - \delta_{18} X_{\rm BHT}^{\rm II}, \\
\theta_2 \frac{S_{\rm O}^{\rm II}}{\delta_6 + S_{\rm O}^{\rm II}} X_{\rm BHT}^{\rm II} &= \theta_3 \left(\delta_{22} - S_{\rm O}^{\rm II}\right).
\end{aligned} \tag{8}$$

We do not pursue to solve the system of equations (8) here, and confine ourselves instead to considering the system's qualitative behavior. It is clear, that the growth of the biomass is not limited by the availability of $S_{\rm S}$, and that hydrolysis is not limited by the availability of $X_{\rm S}$. However, both biomass growth and hydrolysis do depend on the available dissolved oxygen here.

From $(8)_1$, it is clear that $dS_{\rm S}^{\rm II}/dt \leq 0$ for $\delta_4 > \delta_9$, or, in dimensional terms, $\mu_{\rm HT}/Y_{\rm HT} > k_{\rm HT}$. This corresponds to the case of $S_{\rm S}$ being consumed faster by the biomass than it is generated by hydrolysis. We restrict our discussion here to this case. For this case, there is $t_{\rm S} = \mathcal{O}(1)$ such that $S_{\rm S}^{\rm II}(t_{\rm S}) = 0$, and this indicates a region that we will discuss next.

3.5 Region III, $t^* = \mathcal{O}(1)$

This time-scale corresponds to $t^* = \mathcal{O}(1)$ where $t = t_{\rm S} + \varepsilon t^*$, and gives the location of a region where the availability of $S_{\rm S}$ becomes a limiting factor in the further growth of the biomass. Also, the oxygen concentration undergoes a rapid change over this time-scale. In our numerical solutions (see Fig. 7(b)), $t = t_{\rm S}$ gives the time when the biomass $X_{\rm BHT}$ achieves its maximum. For $t^* = \mathcal{O}(1)$, we have

$$X_{\rm S} \sim X_{\rm S}^{\rm II}(t_{\rm S}),\ X_{\rm BHT} \sim X_{\rm BHT}^{\rm II}(t_{\rm S}),$$

where both these quantities are determined as part of the solution to the leading order problem in Region II. In $t^* = \mathcal{O}(1)$, we pose

$$S_{\rm S} \sim \varepsilon S_{\rm S}^{\rm III}(t^*),\ S_{\rm O} \sim S_{\rm O}^{\rm III}(t^*),$$

to obtain

$$\begin{aligned}
\frac{dS_{\rm S}^{\rm III}}{dt^*} &= -\delta_4 \frac{S_{\rm S}^{\rm III}}{1 + S_{\rm S}^{\rm III}} \frac{S_{\rm O}^{\rm III}}{\delta_6 + S_{\rm O}^{\rm III}} X_{\rm BHT}^{\rm II}(t_{\rm S}) + \delta_9 \frac{S_{\rm O}^{\rm III}}{\delta_6 + S_{\rm O}^{\rm III}} X_{\rm BHT}^{\rm II}(t_{\rm S}), \\
\frac{dS_{\rm O}^{\rm III}}{dt^*} &= -\theta_2 \frac{S_{\rm S}^{\rm III}}{1 + S_{\rm S}^{\rm III}} \frac{S_{\rm O}^{\rm III}}{\delta_6 + S_{\rm O}^{\rm III}} X_{\rm BHT}^{\rm II}(t_{\rm S}) + \theta_3 \left(\delta_{22} - S_{\rm O}^{\rm III}\right).
\end{aligned} \tag{9}$$

As $t^* \to \infty$, $dS_{\rm S}^{\rm III}/dt^* \to 0$, $dS_{\rm O}^{\rm III}/dt^* \to 0$, $S_{\rm S}^{\rm III} \to \rho_2$, $S_{\rm O}^{\rm III} \to \rho_3$, where

$$\rho_2 = \frac{\delta_9}{\delta_4 - \delta_9},$$

(recall that we are considering $\delta_4 > \delta_9$ here), and

$$\rho_3 = \frac{1}{2}\left[\delta_{22} - \delta_6 - \frac{\theta_2}{\theta_3}\frac{\delta_9}{\delta_4}X^{\mathrm{II}}_{\mathrm{BHT}}(t_{\mathrm{S}}) + \sqrt{\left(\delta_{22} - \delta_6 - \frac{\theta_2}{\theta_3}\frac{\delta_9}{\delta_4}X^{\mathrm{II}}_{\mathrm{BHT}}(t_{\mathrm{S}})\right)^2 + 4\delta_{22}\delta_6}\right].$$

These predictions are in good agreement with the numerical solution displayed in Fig. 7(a).

3.6 Region IV, $t = \mathcal{O}(1), t_{\mathbf{S}} < t < t_{\mathbf{X}}$

This is the time-scale that starts when most of S_{S} that was initially available is used up and ends at the moment t_{X} when most of the X_{S} is degraded. In this region, we have

$$S_{\mathrm{S}} \sim \varepsilon\frac{\delta_9}{\delta_4 - \delta_9},$$

and we have $X_{\mathrm{S}}, X_{\mathrm{BHT}}, S_{\mathrm{O}} = \mathcal{O}(1)$. For brevity, we do not display or discuss the leading order equations here, and simply note that there is a $t_{\mathrm{X}} = \mathcal{O}(1)$ such that $X_{\mathrm{S}}(t_{\mathrm{X}}) = 0$, which determines the time when the availability of X_{S} first becomes a limiting factor for hydrolysis.

We omit discussion of Regions V and VI, other than to give their locations and the scalings. This is because typical batch times are in the order of 1 day and the behavior of the regions V and VI cannot be observed in these short times. Consequently, these regions are of no practical relevance as for example, all the biomass dies out. Region V is located at $t^\dagger = \mathcal{O}(1)$, where $t = t_{\mathrm{X}} + \varepsilon t^\dagger$, and in which $S_{\mathrm{S}}, X_{\mathrm{S}} = \mathcal{O}(\varepsilon)$, $X_{\mathrm{BHT}}, S_{\mathrm{O}} = \mathcal{O}(1)$. Region VI is at $t = \mathcal{O}(1), t > t_{\mathrm{X}}$ and here we also have $S_{\mathrm{S}}, X_{\mathrm{S}} = \mathcal{O}(\varepsilon)$, $X_{\mathrm{BHT}}, S_{\mathrm{O}} = \mathcal{O}(1)$.

4 Our Approach

As with many biological systems, there is considerable uncertainty in inferring both the functional description of processes and the accuracy of parameterizations when applying laboratory-derived models to the real system. The current models in the wastewater literature are motivated by microbiological and engineering interest and have been devised to incorporate as much as possible of the apparent understanding of underlying processes. As a result they tend to include a relatively large number of variables, processes, and parameters.

This stands in contrast to the scarcity of data accessible from ATAD plants in operation: aeration rate and sludge temperature are easily monitored, but data on sludge composition at inlet and outlet and during the course of the batch reaction is typically limited to the total dry weight of solids and the chemical oxygen demand of the 'volatile solids' (by controlled chemical oxidation of the sludge). Volatile solids include the biomass of bacteria in the sludge together with organic growth substrates and metabolically inert organic compounds, so no distinction is made between these components in the measured data.

The full ASM1 model has large numbers of variables and interactions, and consequently many parameters. The motivation for including these in the model is predominantly microbiological,

and seems to arise from the urge to include all possible components about which there is some knowledge. However, many of the parameter values are poorly known: they are dependent on the chemical and microbiological make-up of the particular sludge, and therefore typically used as fitting parameters. With such a highly parameterized model, sets of parameter values can be found to fit most data but it is unclear if the model remains reliable in such situations. Applying a parameterized model under different (but physically reasonable) operating conditions may give spurious modeling artifacts. And this may also cause numerical difficulties in attempting any optimization.

These considerations motivate us to seek a minimal model which should be capable of describing the essential mechanisms of the ATAD process, but ignore issues which — though microbiologically 'known' — are not material to the process within the likely range of operating conditions. It is hoped that such a model might describe the process sufficiently accurately while providing a more suitable basis for optimization.

4.1 Basic Modeling Assumptions

Some simplifying assumptions permit us to reduce the complexity of the model while at the same time retaining the essential aspects of the processes:

1. There is complete mixing inside the reactor(s).

2. All the biological activity takes place only in the reactors.

3. The batch outflow and inflow stages are of sufficiently short duration that biological activity during them is negligible.

4. Aeration is sufficient that anaerobic metabolic activity is negligible.

As indicated in our analysis of the ASM1 model, we opt to ignore the presence of mesophiles since the mixed sludge is hot enough to render their metabolic activity negligible. A biomass concentration variable X_{B} corresponds to the concentration of thermophiles in the sludge. Any mesophiles in the inflow sludge can effectively be considered as already lyzed into additional contributions to substrate and inerts.

We also choose to ignore the distinction between the two pools of substrate S_{S} and X_{S}, and consider a single substrate pool X. This is motivated by the urge to simplify to a minimal model, rather than through an assumption that one or other pool may be neglected because it is never rate-limiting under normal operating conditions. The effect of this simplification is greatest after substrate is depleted and becomes limiting (e.g. from Region III of Fig. 7(a) in the ASM1 model): in our model substrate availability for metabolism is directly dependent on biomass decay, while in the ASM1 model it is buffered by the slow substrate reservoir. The size of this effect remains to be demonstrated as well as its importance in relation to achieving the treatment goals.

For a single batch and a single reactor, we introduce the following governing ordinary differential equations,

$$\begin{aligned} \frac{dX_{\mathrm{B}}}{dt} &= G - b(T)X_{\mathrm{B}}, \\ \frac{dX}{dt} &= -\alpha G + b(T)(1-f)X_{\mathrm{B}}, \\ \frac{dS}{dt} &= A(\bar{S} - S) - \beta G, \\ \frac{dT}{dt} &= \lambda G - h(T), \end{aligned} \tag{10}$$

where biomass concentration $X_{\mathrm{B}}(t)$ has units [g/l], substrate concentration $X(t)$ has units [g/l], $S(t)$ is the oxygen concentration [g/l][1], and $T(t)$ is temperature [°C]. Biomass is assumed here to have a growth rate G given by the dual Michaelis–Menten kinetics expression

$$G = \mu(T)\frac{S}{K_s + S}\frac{X}{K_x + X}X_{\mathrm{B}}. \tag{11}$$

The biomass is also subject to linear decay with rate constant b which may be temperature-dependent. Growth of biomass is proportional to the substrate and oxygen consumptions with the consumption efficiency $1/\alpha$ and $1/\beta$ respectively. Substrate X is also produced as a result of decay of biomass, of which a fraction $(1-f)$ is recycled as substrate.

Dissolved oxygen is replenished through aeration that is subject to the saturation concentration $\bar{S}$. The sludge temperature increases at a rate proportional to the biomass growth rate and is decreased by heat loss from the reactor. This heat loss occurs through the reactor walls, via the exhaust gas stream from aeration and in the sludge outflow. The heat loss is dominated by losses through latent heat of evaporation in the exhaust gas stream. And while the other heat loss pathways are proportional to $T - T_{\mathrm{amb}}$, this heat loss pathway is less temperature-dependent so we model it with a simple constant loss rate.

The parameters for this model are summarized in Table 3. Most of the parameters relate to the thermophile metabolism and sludge properties alone, but those dependent on reactor design are aeration A, heating rate coefficient λ, and heat loss rate h. In the lack of specific plant information, it was deemed appropriate at this stage to focus on operating conditions rather than plant design in any optimization approaches.

This model describes the batch reaction period from just after a batch intake is mixed into the reactor until batch outflow. The required initial conditions are those of the sludge immediately following mixing of the inflow with the sludge remaining in the reactor from the previous batch, since the reactor volume is only partially replaced at each batch. The pre-existing sludge conditions depend on the history of previous batches in the reactor. With repeated batches of the same type, we expect the batch cycle to settle to state in which successive batches are identical and the pre-mixing reactor sludge conditions are effectively independent of the initial conditions of the first

[1]Note that the units [mg/l] are normally used as a conventional way in wastewater treatment.

Table 3: *Set of parameters for the derived ATAD model.*

Symbol	Description	Value	Units	Reference
	Physical parameters			
K_x	half-saturation constant for substrate	0.1	g/l	[3]
K_s	half-saturation constant for oxygen	0.00017	g/l	"
μ	growth rate	10	1/d	"
b	decay rate	5	1/d	"
α	substrate transformation	1.5	–	"
β	oxygen transformation	0.5	–	"
λ	heat production	6.5	^{o}C[l/g]	"
h	heat loss rate	7	^{o}C/d	–
$\bar{S}$	oxygen saturation constant	0.01	g/l	–
	Baseline case parameters			
A	aeration rate	200	1/d	[3]
$X_{\mathrm{B}}^{\mathrm{feed}}$	biomass input/feeding rate	1	g/l	"
X^{feed}	sludge input/feeding rate	15	g/l	"
S^{feed}	oxygen input/feeding rate	0.001	g/l	"
V_{in}/V	ratio of volume input	0.1	–	"
T^{feed}	temperature of the feed	13	^{o}C	–

batch reactor sludge. We therefore provide initial conditions for the inflow sludge added at each batch and also reactor sludge initial conditions for the first batch. The model can be run to simulate successive batches until these settle to a periodic batch cycle, as indicated in Fig. 8. The linking of successive batches and initial mixing of inflow sludge for each batch can be described by adding additional terms into the system:

$$\begin{aligned} \frac{dX_{\mathrm{B}}}{dt} &= G - bX_{\mathrm{B}} + Q_\delta(X_{\mathrm{B}}^{\mathrm{feed}} - X_{\mathrm{B}}), \\ \frac{dX}{dt} &= -\alpha G + b(1-f)X_{\mathrm{B}} + Q_\delta(X^{\mathrm{feed}} - X), \\ \frac{dS}{dt} &= A(\bar{S} - S) - \beta G + Q_\delta(S^{\mathrm{feed}} - S), \\ \frac{dT}{dt} &= \lambda G - h + Q_\delta(T^{\mathrm{feed}} - T), \end{aligned} \tag{12}$$

where we define the Q_δ as

$$Q_\delta = \frac{V_{\mathrm{in}}}{V}\delta(t - t_{\mathrm{in}}),$$

and $\delta(t - t_{\mathrm{in}})$ is a Dirac delta function.

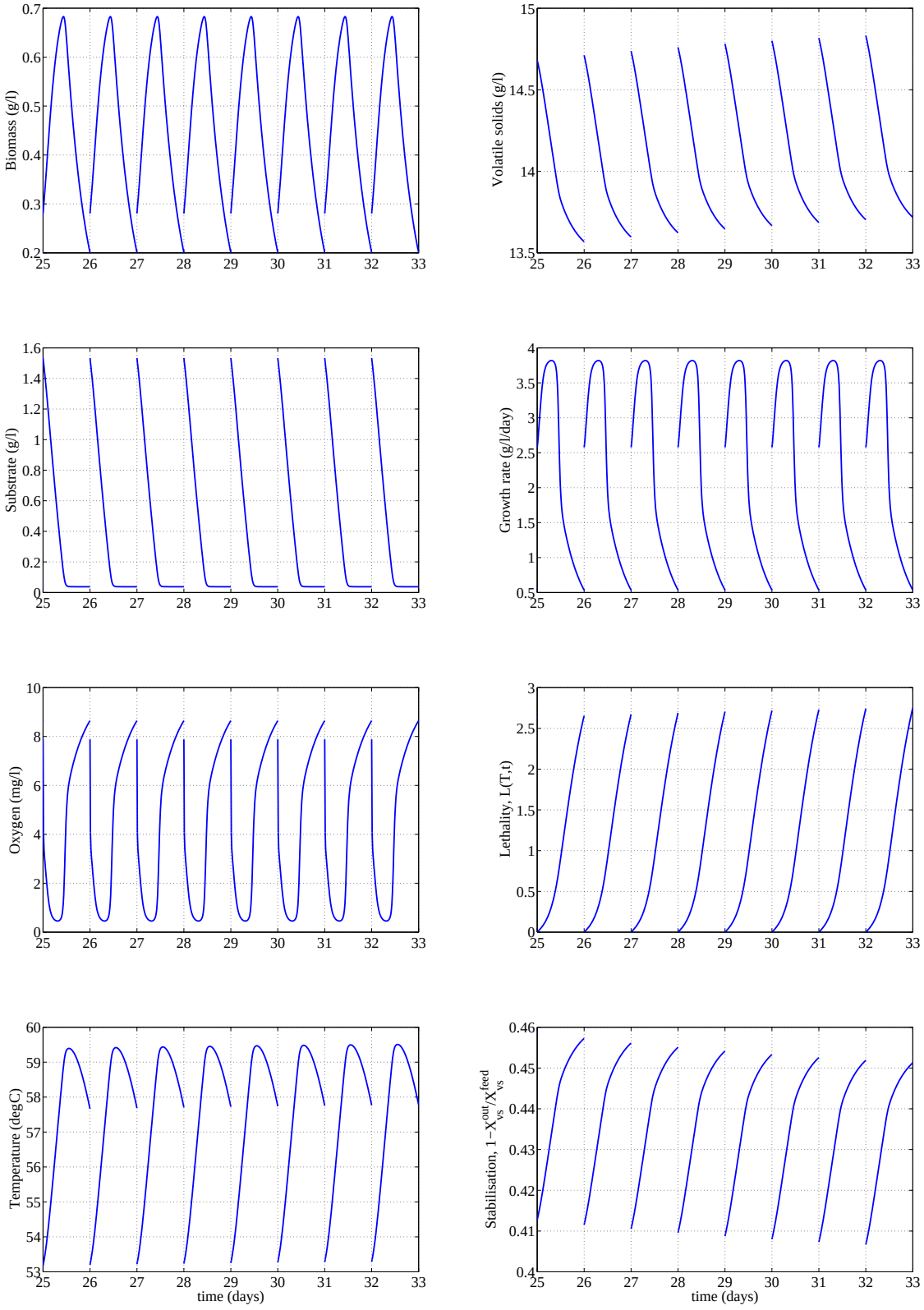

Figure 8: *Multiple batch steady-state numerical simulations of the derived ATAD model.*

The treatment goals for stabilization and pasteurization can be calculated at any solution time after solving the system up to that time. The stabilization target (1) is defined in terms of the volatile solids X_{vs}, which can be calculated by integrating

$$\frac{dX_{\text{vs}}}{dt} = G(1-\alpha) + Q_\delta(X_{\text{vs}}^{\text{feed}} - X_{\text{vs}}). \tag{13}$$

The pasteurization target can be calculated by performing the integration (2) while $T \geq 50^{\text{o}}\text{C}$ and setting $L = 0$ at other times.

Our first approach is to neglect the temperature dependence of the parameters so that the temperature equation decouples from the system. We choose values corresponding to temperature $T = 50^{\text{o}}\text{C}$. As typically ATAD operates at temperatures are higher than 45^{o}C, one may note from Fig. 1 that this assumption tends to give overestimates of biomass growth and temperature.

5 Numerical Simulations

The derived model consists of a system of first order ordinary differential equations which are integrated in time using *Matlab's* stiff solver, *ODE15s*. We validate and test the practical applicability of the model by comparing the numerical simulations with experimental data for a specific choice of parameters given in Table 3. A comparison between the experimental data and numerical simulations is given in Figs. 10 and 11 for dynamical operational conditions, i.e., the input volume is not the same for each batch, cf. [4]. Note that here we ignore any temperature dependence of the kinetic parameters. Despite the limitations in the available data, the comparison shows a very good fit.

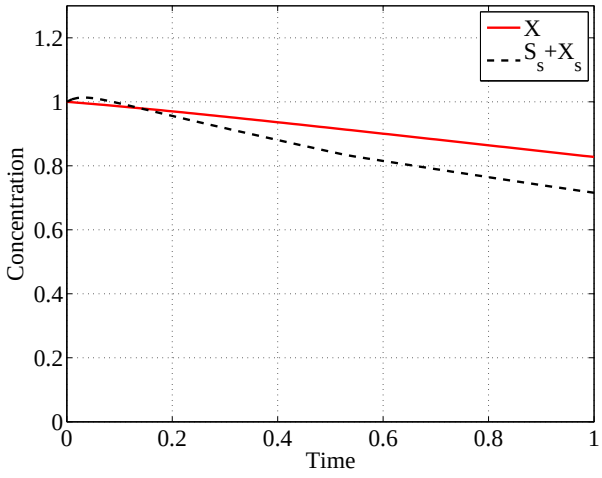

Figure 9: *A comparison between the ASM1 substrate pools S_S+X_S and the substrate X of the simplified model.*

One of the major simplifications of the reduced model is the combination of the two substrate pools S_{S} and X_{S} into one single substrate X. Therefore to show the substrate dynamics of the two

models, Fig. 9 displays the nondimesionalized concentrations of $S_S + X_S$ and X during the first batch of the ASM1 model and the reduced model, respectively. As it can be seen, the difference between the two models in terms of substrate evolution is not significant.

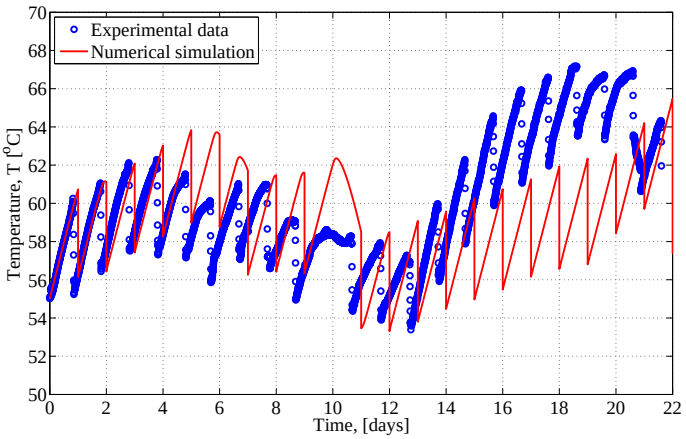

Figure 10: *A comparison between experimental data and numerical simulations of the derived ATAD model for multiple batches (adapted from [3]).*

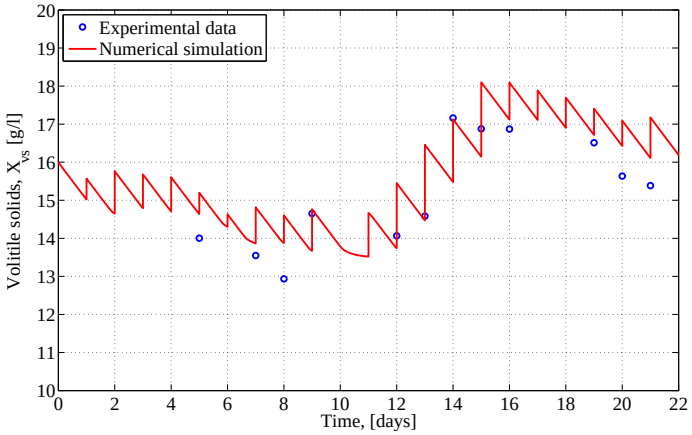

Figure 11: *A comparison between experimental data and numerical simulations of the derived ATAD model for multiple batches. (adapted from [3])*

Here we run the simulations until stabilization (see equation (1)) is achieved. This occurs within day 33 using the baseline case parameters. The numerical simulations for a base case run (and multiple batches) are shown in Fig. 8 where all the parameters are fixed as given in Table 3. Results presented here are for a single reactor and for completeness we also show simulations for pasteurization (see equation (2)).

5.1 Sensitivity Analysis

Here we will consider the variation of the treatment goals on the feed temperature, sludge feed concentration and aeration rate. The simulations in Figs. 12, 13 and 14 are for the 33^{rd} batch with a duration of 1 day. The baseline case simulations are highlighted with an asterisk in the figures.

5.1.1 Sensitivity to the Feed Temperature, $T^{\mathbf{feed}}$

In this section, we study the sensitivity of the model to variations of feed temperature to investigate the impact of this on the bio-treatment goals, i.e., pasteurization and stabilization. This, in practice, can be achieved by preheating fresh sludge before loading into the reactor using recovered heat. We observe from Fig. 12 that, for a given set of parameters, stabilization is not sensitive to the feed temperature. However, pasteurization is very sensitive to feed temperature which is consistent with plants with more than one reactor.

Note the discontinuity in Fig. 12(a). This is because lethality, as defined by equation (2), is nonzero when the temperature is above or equal to 50°C and zero otherwise. We also note that the lack of variation in Fig. 12(b) may be a direct result of using temperature independent parameters.

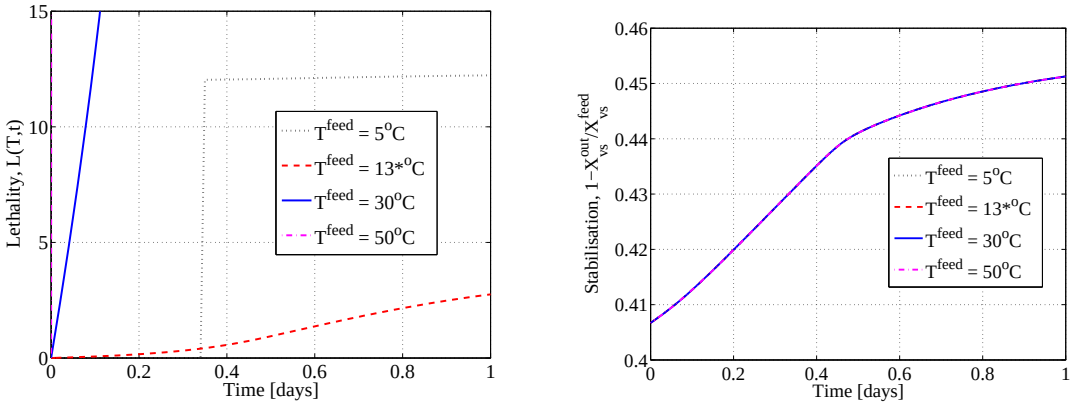

Figure 12: *Lethality and stabilization for different feed temperatures.*

5.1.2 Sensitivity to Sludge Feed, $X^{\mathbf{feed}}$

In this section we consider variations of the sludge feeding pattern to investigate the impact of this on the bio-treatment goals. Fig. 13 suggests the organic feed must be within certain concentrations to attain the required levels of pasteurization and stabilization.

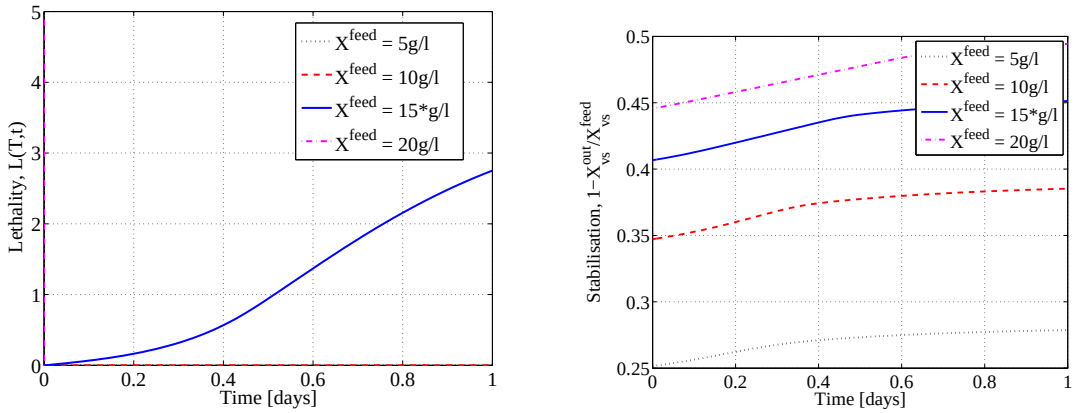

Figure 13: *Lethality and stabilization for different sludge feed concentration.*

5.1.3 Sensitivity to Aeration Rate, A

Since there is some uncertainty in the choice of the aeration rate, we run numerical simulations for different values of A. In fact it is an open question whether continuous aeration is necessary (such as in the Killarney plant). Numerical results (for a single reactor) suggest that the required treatment goals cannot be achieved for aeration rate lower that 100 1/d, see Fig. 14.

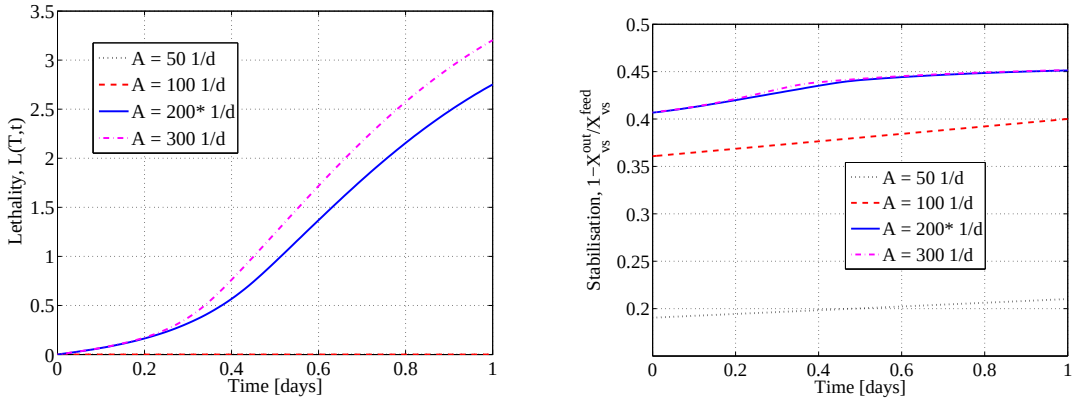

Figure 14: *Lethality and stabilization for different aeration rates.*

5.2 Sensitivity to Oxygen Feed, S^{feed}

In this section we consider varying the oxygen feed concentration. We run simulations for values in the range $S^{\text{feed}} = [0.01 - 10]\,\text{mg/l}$ and results (not shown here) suggest stabilization and pasteurization are not sensitive to the oxygen feed concentration. This suggests that the plant can operate efficiently at levels lower than $S^{\text{feed}} = 1.0\,\text{mg/l}$ while maintaining the required treatment goals.

6 Optimization

The objective of our optimization problem is to minimize the energy consumed per mass of treated sludge by altering the operating conditions while complying with treatment goals (stabilization and pasteurization). Dynamic optimization (also called 'open loop optimal control') is the methodology required to solve this problem due to the time-dependent (semi-batch) nature of the ATAD reaction. There are some recent review papers on dynamic optimization in the context of chemical engineering, [1, 2]. Dynamic optimization requires a dynamic model of the reaction kinetics, and for this purpose we have developed the ATAD model presented herein. It is noteworthy, that this model, in contrast to all the other models present in the available literature, is the only one to quantify both treatment goals (stabilization and pasteurization, see equations (1) and (2)), thus allowing to precisely determine the minimum time and energy needed to comply with legal requirements. This aspect of the model is critical for the purpose of our work, thus paving the way for the optimization problem. The optimization problem in question can be formulated as follows:

$$\min_{\mathbf{u}(t),t_f} E_m[\mathbf{x},\mathbf{u}] = \frac{1}{m_{\text{feed}}}\int_{t_0}^{t_f} P(\mathbf{u}(s))ds, \tag{14}$$

subject to

$$f(\dot{\mathbf{x}},\mathbf{x},\mathbf{u}) = 0, \tag{15}$$

$$\mathbf{x}(t_0) = \mathbf{x}_0, \tag{16}$$

$$0.38 - r_{\text{vs}}(t_f) \leq 0, \tag{17}$$

$$1 - L(t_f) \leq 0, \tag{18}$$

$$\mathbf{u}_L \leq \mathbf{u}(t) \leq \mathbf{u}_v, \tag{19}$$

where E_m is the gravimetric energy requirement [kWh/kg] of volatile solids (VS) treated, m_{feed} is the total mass of VS in the influent [kg], t_0 and t_f are the initial and final time [d], respectively, P is the power of the aeration equipment [kW], $\mathbf{x}(t)$ and $\mathbf{u}(t)$ are the state and optimization variables, respectively, r_{vs} is the VS reduction [%], and L is the pasteurization lethality [%].

In our problem, the objective function to be minimized is E_m (see equation (14)). We seek the optimum trajectories of the optimization variables $\mathbf{u}(t)$ that minimizes E_m. Equation (15) represents the set of differential equations (see equation (12)) describing the dynamics of the ATAD reaction which is subject to the initial value problem in equation (16). Equations (17) and (18) (see equations (1) and (2)) express the so-called path constraints and they represent the stabilization and pasteurization constraints, respectively. They ensure that a minimum required level of stabilization and pasteurization is achieved by the end of the reaction. Equation (19) sets the lower and upper boundaries of the optimization variables. In our previous work, we found that the aeration flow rate, sludge flow rate, and feed temperature are the most significant optimization variables, [14].

The problem represented by equations (14)–(19) represents a nonlinear programming problem with differential and algebraic constraints. It is important to note that in this optimization problem

the objective function (or cost functional) is not a tractable function in the sense that it is not explicit. The objective function is rather implicit as it depends on the dynamics described by equation (15). It is after each simulation (and after the dynamics has "unfolded") that we can evaluate the objective function and the feasibility of the solution. The feasibility of the solution depends on whether the path constraints defined by equations (17) and (18) are satisfied.

Having presented the necessary ATAD model, equations (12), and formulated the optimization problem (equations (14)–(19)) we have paved the way for the optimization of the ATAD reaction. The implementation of the problem is currently in progress and will be addressed in a future publication.

7 Concluding remarks

The aim of this paper was to examine the fundamental dynamics of the existing ASM1 model at thermophilic temperatures [9], [14], so as to develop a simplified version of the model that can be used for optimization purposes.

In the analysis of the ASM1 model at thermophilic temperatures, two different regimes were observed, namely, when either oxygen, or the substrate (the nutrient) are limiting factors to the growth of thermophilic microorganisms. The study of the system behavior has given an important insight into the nature of the process and has enabled us to give a number of practically relevant recommendations, see for example appendices A and B. We have noted that existing ATAD models are greatly oversized, while the reliable data are rather scarce. Furthermore, the existing models are very sensitive to the parameter values. Therefore, we suggested that under this circumstance a simpler model is needed.

Having in mind the optimization of ATAD systems as our ultimate goal, the development of a simple and computationally efficient model was critical. In this context, a simplified model of the ATAD reaction was developed. The model in question includes only the essence of the process. It contains four crucial variables, namely, the substrate concentration (the nutrient), biomass concentration, oxygen concentration, and the temperature of the sludge. The model describes the process of bio-treatment for the case of a single reactor. It has been shown, that for correctly re-calibrated parameters our model and the original large-scale models give effectively the same outcome. Development and verification of this model was the major outcome of this study.

A general optimization problem of the ATAD reaction was formulated. The simplified model and the optimization formulation pave the way for the implementation of the optimization of ATAD systems. The optimization problem formulated above is being implemented and will be addressed in a future publication.

In future, we will also estimate some of the parameters for the reduced model by fitting with existing experimental data.

Acknowledgement:
This industrial problem was presented at the 70^{th} European Study Group with Industry (ESGI). We acknowledge the support of the Mathematics Applications Consortium for Science and Industry (www.macsi.ul.ie) funded by the Science Foundation Ireland mathematics initiative grant 06/MI/005.

References

[1] J. R. Banga, E. Balsa-Canto, and C. G. Moles, *Dynamic optimization of bioreactors – a review*, Proc. Ind. Natl. Sci. Acad. **69A** (2003), 257–265. 56

[2] D. Bonvin, S. Palanki, and B. Srinivasan, *Dynamic Optimization of Batch Processes: I. Characterization of the nominal solution*, Comput. Chem. Engin. (2003), 1–26. 56

[3] J. M. Gómez, *Digestión Aerobic Termófila Autosostenida (atad) de fangos. Estudio experimental a escala real y modelización matemática del reactor*, Ph.D. thesis, Universidad de Navarra, San Sebastiña, Spain, Octubre 2007. 50, 53

[4] J. M. Gómez, M. de Gracia, E. Ayesa, and J. L. Garcia-Heras, *Mathematical modelling of Autothermal Thermophilic Aerobic Digesters*, Water Res. **41** (2007), 1859–1872. 35, 37, 52

[5] W. Gujer, M. Henze, T. Mino, T. Matsuo, M. C. Wentzel, and G. R. Marais, *The Activated Sludge Model No. 2: biological phosphorus removal*, Water Sci. Technol. **31** (1995), no. 2, 1–11. 35

[6] W. Gujer, M. Henze, T. Mino, and M. van Loosdrecht, *Activated Sludge Model No. 3*, Water Sci. Technol. **39** (1999), no. 1, 183–193. 35

[7] M. Henze, C. P. L. Grady Jr., W. Gujer, G. R. Marais, and T. Matsuo, *Activated Sludge Model No. 1*, IAWPRC, London, 1987. 35

[8] R. Kovács and P. Mihältz, *Untersuchungen der kinetik der aerob-thermophilen klaerschlammstabilisierung - einfluss der temperatur, 17. Fruehlingsakademie und Expertentagung. Balatonfuered, Germany*, May, 2005. 35, 37, 40

[9] R. Kovács, P. Mihältz, and Z. Csikor, *Kinetics of Autothermal Thermophilic Aerobic digestion: Application and extension of activated sludge model no. 1 at thermophilic temperatures*, Water Sci. Technol. **56** (2007), no. 9, 137–145. 35, 36, 39, 57

[10] T. M. LaPara and J. E. Alleman, *Thermophilic aerobic biological wastewater treatment*, Water Res. **33** (1999), no. 4, 895–908. 35

[11] N. M. Layden, *An evaluation of Autothermal Thermophilic Aerobic Digestion (ATAD) of municipal sludge in Ireland*, J. Environ. Eng. Sci. **6** (2007), 19–29. 36, 38

[12] N. M. Layden, H. G. Kelly, D. S. Mavin, R. Moles, and J. Barlet, *Autothermal thermophilic aerobic digestion (ATAD) – Part I: Review of origins, design, and process operation*, J. Environ. Eng. Sci. **6** (2007), 665–678. 35

[13] ———, *Autothermal thermophilic aerobic digestion (ATAD) – Part I: Review of research and full-scale operating experiences*, J. Environ. Eng. Sci. **6** (2007), 679–690. 35

[14] J. Rojas, T. Zhelev, and A. D. Bojarski, *Modelling and sensitivity analysis of ATAD*, Comput. Chem. Engin. (2009). 36, 56, 57

[15] J. Rojas, T. Zhelev, and M. Graells, *Energy efficiency optimization of wastewater treatment – Study of ATAD*, 2010.

[16] USEPA, *'40 CFR Part 503, standards for the use or disposal of sewage sludge'. United States Environmental Protection Agency, Office of Research and Development, Washington, D.C.*, 1993. 38, 39, 62

Appendix

A Notes on Optimization

The main operating optimization controls are the aeration rate A, the exchanged volume fraction Q, and the batch reaction time t_{batch}. The inflow sludge properties are largely fixed by the nature of the waste rather than being optimization controls. The exception to this is the possibility of enriching the inflow with additional substrate.

Operational restrictions mean that the aeration rate is generally fixed as constant throughout a batch and the batch time is fixed to give a daily cycle. If we adhere to these restrictions, the controls are reduced to the constant aeration rate A and the exchanged volume fraction Q, and optimization will correspond to the treatment goals being achieved at the end of the daily cycle. In this situation, the energy consumption per mass of treated sludge is proportional to A/Q.

The effect of aeration rate A is apparently straightforward: additional oxygenation promotes faster biomass growth and therefore quicker stabilization and temperature increase, giving quicker pasteurization. For a fixed batch time and an exchanged volume fraction, we would reduce the aeration rate until the more stringent treatment goal is achieved at the end of the batch. While energy consumption increases linearly with aeration rate, the growth rate's increase with oxygenation is less than linear, approaching linearity near zero oxygen concentration. This would suggest that it may be desirable to maintain the lowest aeration rate which provides sufficient mixing and limits anaerobic metabolism, though other considerations such as plant throughput may become overriding.

The effect of the exchanged volume fraction Q is less clear. The inflow sludge brings new substrate into the reactor, which leads to increased growth rate, digestion, and heating. However,

it also cools the sludge mixture which slows the pasteurization process. These two effects have competing impacts on the time to achieve the pasteurization goal. The stabilization treatment goal is expressed in terms of the reduction of volatile solids between inflow and outflow (which is extracted directly from the reactor sludge mixture). Similarly, while inflow brings fresh substrate to fuel the metabolism and promote growth, increasing the exchanged fraction also decreases the apparent stabilization just after inflow mixing which can be expressed as $(1 - Q)(1 - X^*_{\text{vs}}/X^{\text{feed}}_{\text{vs}})$, where X^*_{vs} relates to the pre-mixing reactor sludge remaining from the previous batch.

A typical ATAD batch reaction follows a timecourse similar to that shown in Fig. 6(a). The influx of new substrate on initial mixing leads to a rapid increase in metabolic activity and concomitant depletion of oxygen. Substrate is initially in abundance and is digested through the batch reaction, while oxygen is constantly supplied through aeration. At the start of a batch reaction oxygen rapidly becomes limiting while the substrate remains abundant. In this phase the biomass growth rate is mostly determined by the aeration rate and is largely independent of the substrate. As substrate concentration starts to become depleted the control of the process transfers to the diminishing substrate level.

The effect of inflow substrate enrichment is to delay the depletion of substrate, extending the duration of the initial oxygen-depleted phase. It has minimal effect on the growth rate or temperature (and hence treatment goals) until the time at which substrate would otherwise have started to become limiting. As substrate enrichment directly increases inflow volatile solids, it means that a greater quantity of volatile solids must be digested to achieve stabilization.

Once substrate is sufficiently depleted that it is limiting, the oxygen level under constant aeration will generally increase. At this stage, additional substrate comes only from biomass decay (in the ASM1 scheme, via the remaining slow substrate pool), so the growth rate must decrease from this point until decay dominates and then finally the temperature will start to drop. It would therefore appear to continue the reaction (and aeration) significantly into the stage of a decreasing reaction rate except to achieve an unsatisfied treatment goal.

As a broad guideline for optimization, it would therefore appear ideal to adjust the aeration rate and exchanged volume fraction so that the substrate should become depleted close to the end of the batch time, and this should coincide with the two treatment goals being achieved. It is uncertain whether this is achievable with just these controls in a fixed plant design. Increasing aeration accelerates both treatment goals, but directly increases energy consumption. Substrate enrichment enhances pasteurization more than stabilization. Increasing exchanged volume fraction probably delays achievement of both treatment goals, though pasteurization may be greater affected if the post-mixing temperature drops significantly; it also decreases energy consumption by increasing the sludge throughput.

B Optimal Strategy for Pasteurization

In this section we provide an alternative discussion of the optimization problem. We mentioned that the treatment has two different Objectives, namely:

1. Killing the pathogen by pasteurization, and
2. Stabilization; that is reducing the organic matter contents to an acceptable level (66–80% of the initial).

However, one can expect that when one of these Objectives is achieved, another is already accomplished in the process as well. For example, when the treated sludge is pasteurized and the pathogen are killed or reduced to safe level, this portion of sludge is also already stabilized (that is the organic content is reduced to an acceptable level). This observation allows us to substitute one difficult problem that has two Objectives by two simple separable problems that have a single Objective each. In this Section we consider an optimal control policy that is aimed to pasteurization, assuming that the stabilization will be reached in the process of pasteurizing.

Pasteurization implies exposing the sludge to high temperature for a prolonged time. To achieve this objective in an optimal way, we may consider a simple practical analogue. The optimal policy for pasteurization will be

1. Firstly, heat the contents to as high as possible temperature, and do it as quickly as possible.
2. After heating, maintain this temperature for the necessary time.

The temperature of the sludge and the heat influx for this process are shown in Fig. 15.

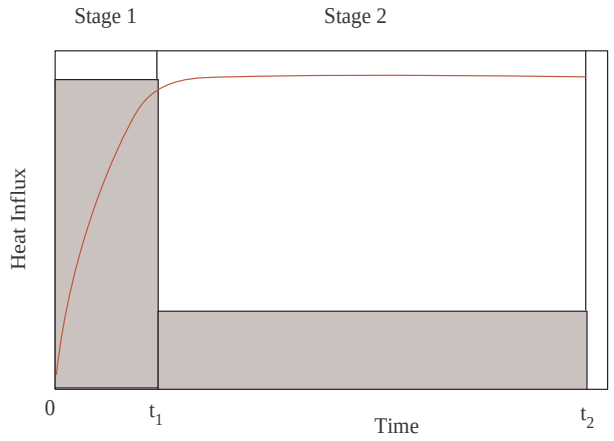

Figure 15: *Sludge temperature (given by the curve) and the proposed heat influx (given by the rectangles).*

This involved four questions, namely:
Question 1: What temperature should the sludge be?

Answer: The temperature should be as high as it can be maintained for a prolonged time. It is obvious that the highest temperature that can be maintained is the temperature when the rate of metabolism balances the bacteria rate of decay (Fig. 16)

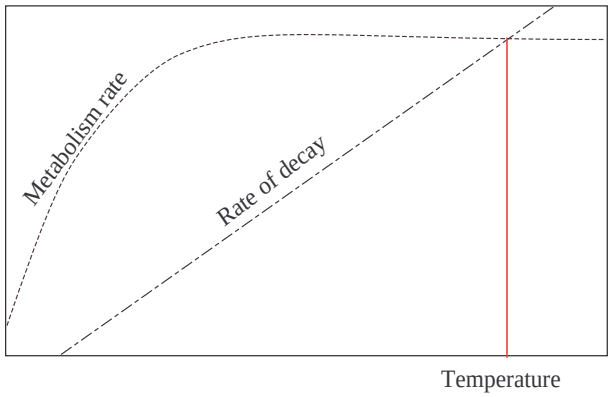

Figure 16: *The equilibrium of the metabolism rate and the rate of decay.*

Question 2: How long should Stage 1 (heating) be?

Answer: As long as needed to reach the pasteurization temperature at the highest possible heating rate

Question 3: How much heat is needed to maintain the temperature through Stage 2?

Answer: By the model,

$$\frac{dT}{dt} = \text{Heat Influx} - \text{Heat Losses}.$$

At equilibrium $dT/dt = 0$, and hence *Heat Influx = Heat Losses*. The heat losses are known for a given temperature, and hence we have the heat influx. For instance, if the heat losses are linearly proportional to the temperature, that is Heat Losses $= hT$, and the heat influx is proportional to the rate of metabolism,

$$\text{Heat Influx} = \mu \frac{S}{K_s + S} \frac{X}{K_x + X} X_{\text{B}}$$

then the task is to maintain the oxygen concentration S at such a level that

$$\frac{S}{K_s + S} \approx 1.$$

Question 4: How long should Stage 2 be?

Answer: As long as needed to reach the required level of pasteurization (this time is well known and is given by a known formula, equation (2) [16]).

B.1 Recommendations

1. Thermal-isolation and utilizing the waste heat. Thermal-isolation reduces heat losses and hence the heat influx can be also reduced.

2. Splitting the process by stages. We suggest that the process should be divided into two stages, namely the heating and the maintaining the temperature. It is advisable to conduct these two processes in different reactors.

3. Preheating the water (utilizing waste heat). Preheating the water would shorten the first stage, the heating and the thermal shock will be smaller.

4. Start every round of the process at the highest possible initial concentration of bacteria. This again should shorten the first stage (the heating) and hence reduce the energy losses.